Latin American Journal of Solids and Structures
www.lajss.org

Free vibration responses of temperature dependent functionally graded curved panels under thermal environment

Abstract

Free vibration responses of shear deformable functionally graded single/doubly curved panels under uniform, linear and nonlinear temperature fields are investigated in the present article. The micromechanical material model of functionally graded material is computed using Voigt model in conjunction with the power-law distribution to achieve the continuous gradation. The material properties are assumed to be the function of temperatures. The mid-plane kinematics of panel geometry is derived using the higher order shear deformation theory. The governing equation of the vibrated panel is obtained using Hamilton's principle. The desired solutions of free vibrated functionally graded shells are computed numerically using the suitable finite element steps. The convergence behaviour of the numerical results has been checked and validated by comparing the responses with that to available published literatura. The applicability of the proposed model has been highlighted by solving various numerical examples for different material and geometrical parameters and temperature fields.

Keywords

Functionally graded materials; free vibration; HSDT; temperature field.

Vishesh Ranjan Kar[a]
Subrata Kumar Panda[b]

[a,b]Department of Mechanical Engineering, NIT Rourkela, Odisha, India

Corresponding author:
[a]visheshkar@gmail.com
[b]call2subrat@gmail.com

http://dx.doi.org/10.1590/1679-78251691

Received 11.11.2014
In revised form 27.04.2015
Accepted 04.05.2015
Available online 07.07.2015

1 INTRODUCTION

The requirement of structural strength in many engineering fields demands the advanced material that can maintain the structural integrity in critical environmental conditions. However, the laminated composites have shown their competencies in many weight sensitivity industries for last few decades. But, besides from this, the layer structures are incapable to sustain their structural integrity due to delamination in the severe thermal environment. In order to bridge the gap, the combination of two dissimilar materials with a continuous variation in transverse direction, known as functionally graded material (FGM), was first proposed by a group of space scientists in Japan (Koizumi, 1993). The capabilities of FGM in combined loading conditions attracted many researchers since last two decades.

Yang and Shen (2003) employed a semi-analytical approach to examine the free vibration and dynamic responses of functionally graded (FG) cylindrical shell under thermal environment by using Reddy's higher-order shear deformation theory (HSDT). Huang and Shen (2004) studied the nonlinear vibration and dynamic response of FG plate in the thermal environment using the HSDT mid-plane kinematics and von Karman type geometric nonlinear strain terms. Sundararajan et al. (2005) employed the first-order shear deformation theory (FSDT) mid-plane kinematics and von-Karman's nonlinearity to obtain nonlinear vibration response of FG plate under thermal environment. Patel et al. (2005) examined the free vibration behaviour of FG cylindrical shells using higher-order kinematics approximation through the thickness. Uymaz and Aydogdu (2007) studied the vibration responses of FG plate for various support conditions by using small strain linear elasticity theory. Haddadpour et al. (2007) investigated frequency responses of simply-supported FG cylindrical shell panel under thermal environment using Love's shell theory and Galerkin's method. Pradyumna and Bandyopadhyay (2008) studied the free vibration behaviour of curved FG panels using the higher-order formulation including Sanders' approximation for the shell panels. Pradyumna and Bandyopadhyay (2010) reported the vibration and buckling behaviour of FG curved panels by including the thermal effect. Santos et al. (2009) obtained the free vibration responses of cylindrical FG shell based on the 3D linear elastic theory by developing a semi-analytical axisymmetric finite element model. Pradyumna et al. (2010) developed higher-order based finite element model to solve the nonlinear transient vibration of FG doubly curved shell panels using New-mark technique. Hosseini-Hashemi et al. (2010) solved the moderately thick FG plate resting on elastic foundations for vibration analysis using the FSDT kinematics with a modified shear correction factor analytically. Talha and Singh (2011) employed the HSDT mid-plane kinematics and Green–Lagrange nonlinear strains to investigate the nonlinear vibration behaviour of FG plate. Rahimia et al. (2011) studied the vibration responses of cylindrical FG shell panel with intermediate ring supports using Sanders' thin shell theory. Alijani et al. (2011a) investigated the nonlinear forced vibration behaviour of the simply-supported FG curved shallow shells using Donnell's nonlinear shallow shell theory. Alijani et al. (2011b) analysed the nonlinear vibration responses of the FG shell panel using the HSDT kinematics including the temperature effect. Baferani et al. (2012) solved analytically the free vibration problem of the FG thin annular sector plates resting on the elastic foundations using Kirchhoff plate theory. Taj and Chakrabarti (2013) presented finite element formulation based on Reddy's higher order theory to investigate the dynamic response of FG skew shell. Pradyumna and Nanda (2013) examined the nonlinear transient behaviour of the FG doubly curved panels with geometrical imperfection under the thermal environment using von-Karman type nonlinear strain terms in the framework of the FSDT mid-plane kinematics. Asemi et al. (2014) presented the static and dynamic behaviour of the FG skew plate based on the 3D elasticity theory. Bich et al. (2014) utilised the FSDT and stress function to investigate the nonlinear dynamic and the free vibration behaviour of imperfect eccentrically stiffened FG thick shallow shells. Shen and Wang (2014) analysed the nonlinear vibration behaviour of the FG cylindrical panel under thermal environment by using the HSDT kinematics with von-Karman nonlinearity. Zhu et al. (2014) performed nonlinear thermo-mechanical analysis of FG plate using local meshless method and Kriging interpolation technique. In their study, the FSDT and von-Karman nonlinearity are used to define the total strain.

The previous studies show that very limited analysis on the free vibration behaviour of the FG single/doubly curved shell panels are reported under thermal environment. The prime objective of the present work to analyse free vibration behaviour of the flat/curved panel of different geometries (flat, cylindrical, spherical, hyperbolic and elliptical) under three different thermal fields (uniform, linear and nonlinear). The FG panel model has been developed based on the HSDT mid-plane kinematics considering the temperature-dependent material properties. The governing equation of the vibrated FG panel is obtained using Hamilton's principle and discretized through suitable finite element steps. The convergence behaviour of the present numerical model has been checked and compared with available published literature. Finally, the effects of different parameters (power-law indices, thickness ratios, aspect ratios, curvature ratios and temperatures) on the frequency responses under different temperature fields are computed using the proposed numerical model and discussed in detailed.

2 GENERAL FORMULATION

In the present study, a general doubly curved shell panel is considered to exhibit all the different shell panels like flat, spherical, cylindrical, hyperbolic and elliptical panels. The dimension and geometry of the doubly curved panel are presented in Figure 1. Here, 'h' is the total thickness of the FG shell panel, and 'a' and 'b' are the sides of the panel along the x and y directions, respectively. The curved panel is defined with respect to the curvature radii. i.e., R_x (along with the x- direction) and R_y (along with the y- direction). The different panel geometries, generated from the doubly curved shell panel, are presented in Table 1.

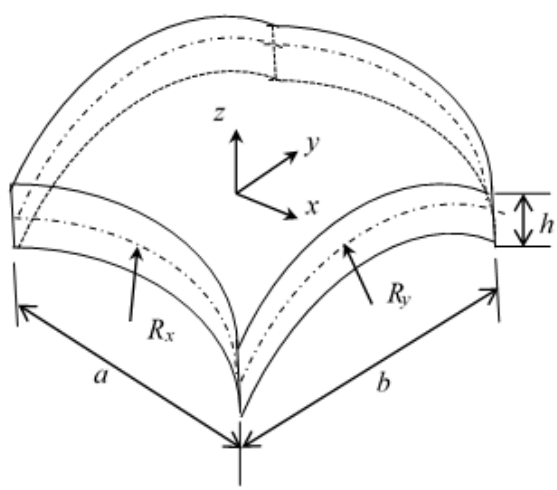

Figure 1: Geometry and dimension of the doubly curved FG shell panel.

Curvature radii	Single/doubly curved shell panel				
	Flat	Spherical	Cylindrical	Hyperbolic	Elliptical
R_x	∞	R	R	R	R
R_y	∞	R	∞	$-R$	$2R$

Table 1: Different shell geometries.

2.1 Kinematic relations

In the present study, the displacements (u,v,w) at any point along the (x,y,z) coordinates in the shell panel are defined in the HSDT mid-plane kinematics with nine degrees of freedom as in Eq. (1) (Pandya and Kant, 1988).

$$\begin{aligned} u(x,y,z,t) &= u_0(x,y,t) + z\theta_x(x,y,t) + z^2u_0^*(x,y,t) + z^3\theta_x^*(x,y,t) \\ v(x,y,z,t) &= v_0(x,y,t) + z\theta_y(x,y,t) + z^2v_0^*(x,y,t) + z^3\theta_y^*(x,y,t) \\ w(x,y,z,t) &= w_0(x,y,t) \end{aligned} \tag{1}$$

where, t is the time. z is the thickness coordinate varies from $-h/2$ to $+h/2$. u_0, v_0 and w_0 are the mid-plane displacements along the x, y and z coordinate, respectively. θ_x and θ_y are the rotations of transverse normal about the y- and x-axis, respectively and other terms are the higher-order terms in the Taylor series expansion defined in the mid-plane of the shell.

Again, Eq. (1) can also be represented in the matrix form as in Eq. (2).

$$\{\delta\} = [f]\{\delta_0\} \tag{2}$$

where, $\{\delta\} = \{u\ v\ w\}^T$, $\{\delta_0\} = [u_0\ \ v_0\ \ w_0\ \ \theta_x\ \ \theta_y\ \ u_0^*\ \ v_0^*\ \ \theta_x^*\ \ \theta_y^*\ ]^T$ and $[f]$ is the function of thickness coordinate matrix and expresses as in Eq. (3).

$$[f] = \begin{bmatrix} 1 & 0 & 0 & z & 0 & z^2 & 0 & z^3 & 0 \\ 0 & 1 & 0 & 0 & z & 0 & z^2 & 0 & z^3 \\ 0 & 0 & 1 & 0 & 0 & 0 & 0 & 0 & 0 \end{bmatrix} \tag{3}$$

2.2 Strain-displacement relations

The strain-displacement relation for doubly curved shell panel can be expressed as (Kar and Panda, 2015)

$$\begin{Bmatrix} \varepsilon_{xx} \\ \varepsilon_{yy} \\ \gamma_{xy} \\ \gamma_{xz} \\ \gamma_{yz} \end{Bmatrix} = \begin{Bmatrix} u_{,x} \\ v_{,y} \\ u_{,y} + v_{,x} \\ u_{,z} + w_{,x} \\ v_{,z} + w_{,y} \end{Bmatrix} = \begin{Bmatrix} \left(\dfrac{\partial u}{\partial x} + \dfrac{w}{R_x}\right) \\ \left(\dfrac{\partial v}{\partial y} + \dfrac{w}{R_y}\right) \\ \left(\dfrac{\partial u}{\partial y} + \dfrac{\partial v}{\partial x} + \dfrac{2w}{R_{xy}}\right) \\ \left(\dfrac{\partial u}{\partial z} + \dfrac{\partial w}{\partial x} - \dfrac{u}{R_x}\right) \\ \left(\dfrac{\partial v}{\partial z} + \dfrac{\partial w}{\partial y} - \dfrac{v}{R_y}\right) \end{Bmatrix} \tag{4}$$

Now, substituting the displacements as in Eq. (1) into Eq. (4), the strain terms can be represented as:

$$\begin{Bmatrix} \varepsilon_{xx} \\ \varepsilon_{yy} \\ \gamma_{xy} \\ \gamma_{xz} \\ \gamma_{yz} \end{Bmatrix} = \begin{Bmatrix} \varepsilon_x^{\,0} \\ \varepsilon_y^{\,0} \\ \varepsilon_{xy}^{\,0} \\ \varepsilon_{xz}^{\,0} \\ \varepsilon_{yz}^{\,0} \end{Bmatrix} + z \begin{Bmatrix} k_x^{\,1} \\ k_y^{\,1} \\ k_{xy}^{\,1} \\ k_{xz}^{\,1} \\ k_{yz}^{\,1} \end{Bmatrix} + z^2 \begin{Bmatrix} k_x^{\,2} \\ k_y^{\,2} \\ k_{xy}^{\,2} \\ k_{xz}^{\,2} \\ k_{yz}^{\,2} \end{Bmatrix} + z^3 \begin{Bmatrix} k_x^{\,3} \\ k_y^{\,3} \\ k_{xy}^{\,3} \\ k_{xz}^{\,3} \\ k_{yz}^{\,3} \end{Bmatrix} \tag{5}$$

where, the strain terms having the superscripts 0, 1, 2, 3 are the extension, bending and the curvature terms at the mid-plane.

Again, Eq. (5) has been rearranged in the following form:

$$\{\varepsilon\} = [T]\{\bar{\varepsilon}\} \tag{6}$$

where, $\{\bar{\varepsilon}\} = \left[\varepsilon_x^{\,0}\ \varepsilon_y^{\,0}\ \varepsilon_{xy}^{\,0}\ \varepsilon_{xz}^{\,0}\ \varepsilon_{yz}^{\,0}\ k_x^{\,1}\ k_y^{\,1}\ k_{xy}^{\,1}\ k_{xz}^{\,1}\ k_{yz}^{\,1}\ k_x^{\,2}\ k_y^{\,2}\ k_{xy}^{\,2}\ k_{xz}^{\,2}\ k_{yz}^{\,2}\ k_x^{\,3}\ k_y^{\,3}\ k_{xy}^{\,3}\ k_{xz}^{\,3}\ k_{yz}^{\,3}\right]^T$ and the individual mid-plane strain terms are presented here in the following line.

$$\varepsilon_x^0 = u_{,x},\ \varepsilon_y^0 = v_{,y},\ \varepsilon_{xy}^0 = u_{,y} + v_{,x},\ \varepsilon_{xz}^0 = w_{,x} + \theta_x,\ \varepsilon_{yz}^0 = w_{,y} + \theta_y,\ k_x^1 = \theta_{x,x},\ k_y^1 = \theta_{y,y},$$

$$k_{xy}^1 = \theta_{x,y} + \theta_{y,x},\ k_{xz}^1 = 2u_0^* - \theta_x \,/\, R_x,\ k_{yz}^1 = 2v_0^* - \theta_y \,/\, R_y,\ k_x^2 = u_{0,x}^*,\ k_y^2 = v_{0,y}^*,\ k_{xy}^2 = u_{0,y}^* + v_{0,x}^*,$$

$$k_{xz}^2 = 3\theta_x^* - u_0^* \,/\, R_x,\ k_{yz}^2 = 3\theta_y^* - v_0^* \,/\, R_y,\ k_x^3 = \theta_{x,x}^*,\ k_y^3 = \theta_{y,y}^*,\ k_{xy}^3 = \theta_{x,y}^* + \theta_{y,x}^*,\ k_{xz}^3 = -\theta_x^* \,/\, R_x,$$

$$k_{yz}^3 = -\theta_y^* \,/\, R_y.$$

$[T] = [I \quad zI \quad z^2I \quad z^3I]$ is the thickness coordinate matrix where I is the identity matrix of size (5×5).

2.3 Effective material properties of FGM

In this study, the bottom and the top surfaces of the FG panel are considered as metal and ceramic rich, respectively. The effective material properties of FGM are considered as functions of temperature and thickness coordinate. The FGM constituents are taken as function of temperature (T) and can be expressed as (Reddy and Chin, 1998)

$$\xi_{c,m}(T) = \xi_0(\xi_{-1}T^{-1} + 1 + \xi_1 T + \xi_2 T^2 + \xi_3 T^3) \tag{7}$$

where, subscript 'c' and 'm' denote ceramic and metal, respectively. ξ_0, ξ_{-1}, ξ_1, ξ_2 and ξ_3 are the temperature coefficients.

The effective material properties of FGM (ξ) can be evaluated by using Voigt's micromechanics model (Gibson et al., 1995) and the power-law distribution (Shen, 2009) expressed as

$$\xi(T,z) = \xi_c(T)\vartheta_c(z) + \xi_m(T)\vartheta_m(z) \tag{8}$$

where, $\vartheta_c\left(z\right)=\left(z/h+1/2\right)^n$ and $\vartheta_m(z)=1-\vartheta_c(z)^n$ are the volume fractions of ceramic and metal, respectively. Here, n denotes the power-law index, ranges from $n=0$ (ceramic rich) to $n=\infty$ (metal rich).

Different material properties such as Young's modulus (E), Poisson's ratio (v), density (ρ), thermal expansion coefficient (a) and thermal conductivity (k) for the FGM constituents are presented in Table 2.

Materials	Properties	ξ_0	ξ_{-1}	ξ_1	ξ_2	ξ_3
	E (Pa)	2.4427E+11	0	-1.3710E-03	1.2140E-06	-3.6810E-10
	α (K^{-1})	12.766E-06	0	-1.4910E-03	1.0060E-05	-6.7780E-11
ZrO_2	v	0.3	0	0	0	0
	k (W/mK)	1.80	0	0	0	0
	ρ (kg/m^3)	3000	0	0	0	0
	E (Pa)	1.2256E+11	0	-4.5860E-04	0	0
	α (K^{-1})	7.5788E-06	0	6.6380E-04	-3.1470E-06	0
$Ti\text{-}6Al\text{-}4V$	v	0.3	0	0	0	0
	k (W/mK)	7.82	0	0	0	0
	ρ (kg/m^3)	4427	0	0	0	0

Table 2: Temperature dependent properties of the FGM constituents (Huang and Shen, 2004).

2.4 Temperature variation across the thickness direction

In order to achieve any general case, three different temperature fields across the thickness direction of the FG panel are considered namely, uniform (TD-I), linear (TD-II) and nonlinear temperature rise (TD-III).

2.4.1 Uniform temperature rise

The temperature field is assumed to be uniform in the thickness direction and the ambient temperature is set as $T_0=300$ K, and the variation of the temperature field is expressed as:

$$T=T_0+\Delta T \tag{9}$$

2.4.2 Linear temperature rise

The linear temperature variation is assumed through the thickness of the FG curved panel and two different temperatures such as T_m and T_c are assumed to be for the metal (bottom) and ceramic (top) rich surfaces, respectively. The temperature field of linear variation through the thickness direction is expressed as:

$$T(z)=T_m+(T_c-T_m)\left(\frac{z}{h}+\frac{1}{2}\right) \tag{10}$$

2.4.3 Nonlinear temperature rise

The FG panel structure is also exposed to the nonlinear temperature variation in the thickness direction and it obtained using the one-dimensional heat conduction equation and expressed as:

$$-\frac{d}{dz}\left(k(z)\frac{dT}{dz}\right)=0 \tag{11}$$

where, $T=T_m$ at the bottom surface ($z=-h/2$) and $T=T_c$ at the top surface ($z=+h/2$). The analytical solution to Eq. (11) is

$$T(z)=T_c-\frac{\left(T_c-T_m\right)}{\left[\int_{-h/2}^{+h/2}\frac{1}{k(z)}\mathrm{d}z\right]}\int_{-h/2}^{z}\frac{1}{k(z)}\mathrm{d}z \tag{12}$$

In Eq. (12), thermal conductivity is considered as the function of thickness coordinate only (Miyamoto et al., 1999). The above equation is again simplified and rewritten as in (Javaheri and Eslami, 2002).

$$T\left(z\right)=T_m+\left(T_c-T_m\right)\times\eta\left(z\right) \tag{13}$$

where,

$$\eta(z)=\frac{1}{C}\left[\left(\frac{z}{h}+\frac{1}{2}\right)-\frac{k_{cm}}{(n+1)k_m}\left(\frac{z}{h}+\frac{1}{2}\right)^{(n+1)}+\frac{k_{cm}^2}{(2n+1)k_m^2}\left(\frac{z}{h}+\frac{1}{2}\right)^{(2n+1)}+\right.$$
$$\left.-\frac{k_{cm}^3}{(3n+1)k_m^3}\left(\frac{z}{h}+\frac{1}{2}\right)^{(3n+1)}+\frac{k_{cm}^4}{(4n+1)k_m^4}\left(\frac{z}{h}+\frac{1}{2}\right)^{(4n+1)}-\frac{k_{cm}^5}{(5n+1)k_m^5}\left(\frac{z}{h}+\frac{1}{2}\right)^{(5n+1)}\right]$$

and

$$C=1-\frac{k_{cm}}{\left(n+1\right)k_m}+\frac{k_{cm}^2}{\left(2n+1\right)k_m^2}-\frac{k_{cm}^3}{\left(3n+1\right)k_m^3}+\frac{k_{cm}^4}{\left(4n+1\right)k_m^4}-\frac{k_{cm}^5}{\left(5n+1\right)k_m^5}$$

where, $k_{cm}=k_c-k_m$.

Eq. (13) can be simplified for the isotropic material (fully metal/ceramic rich) as

$$T(z)=\frac{T_c+T_m}{2}+\frac{T_c-T_m}{h}z \tag{14}$$

2.5 Thermoelastic constitutive relation

The thermoelastic constitutive relations for the FG shell panel are expressed as (Shen, 2009) follows:

$$\begin{Bmatrix}\sigma_{xx}\\ \sigma_{yy}\\ \tau_{xy}\\ \tau_{xz}\\ \tau_{yz}\end{Bmatrix}=\begin{bmatrix}Q_{11} & Q_{12} & 0 & 0 & 0\\ Q_{21} & Q_{22} & 0 & 0 & 0\\ 0 & 0 & Q_{33} & 0 & 0\\ 0 & 0 & 0 & Q_{44} & 0\\ 0 & 0 & 0 & 0 & Q_{55}\end{bmatrix}\left(\begin{Bmatrix}\varepsilon_{xx}\\ \varepsilon_{yy}\\ \gamma_{xy}\\ \gamma_{xz}\\ \gamma_{yz}\end{Bmatrix}-\begin{bmatrix}1\\ 1\\ 0\\ 0\\ 0\end{bmatrix}\alpha\Delta T\right) \tag{15}$$

where, $Q_{11}=Q_{22}=E\Big/\left(1-\upsilon^2\right)$, $Q_{12}=Q_{21}=E\upsilon\Big/\left(1-\upsilon^2\right)$, $Q_{33}=Q_{44}=Q_{55}=E\Big/2\left(1+\upsilon\right)$
Now, Eq. (15) can also be represented as

$$\left\{\sigma\right\}=\left[Q\right]\left\{\varepsilon\right\}-\left[Q\right]\left\{\varepsilon_{th}\right\} \tag{16}$$

where, $\left[Q\right]$ is the stiffness matrix and $\left\{\varepsilon_{th}\right\}=\left[1\ 1\ 0\ 0\ 0\right]^T\alpha\Delta T$ is the thermal strain vector.

The strain energy of the curved shell panel can be expressed as:

$$U=\frac{1}{2}\iint\left[\int_{-h/2}^{+h/2}\left\{\varepsilon\right\}^T\left\{\sigma\right\}\mathrm{d}z\right]\mathrm{d}x\,\mathrm{d}y \tag{17}$$

Eq. (17) can be rewritten by substituting the mid-plane strain vector and the stresses from Eqs. (6) and (16) and conceded as:

$$U=\frac{1}{2}\iint\left(\left\{\varepsilon\right\}^T\left[D\right]\left\{\varepsilon\right\}\right)\mathrm{d}x\,\mathrm{d}y \tag{18}$$

where,

$$\left[D\right]=\int_{-h/2}^{+h/2}\left[T\right]^T\left[Q\right]\left[T\right]\mathrm{d}z\,.$$

The total work done by the membrane forces due to temperature rise across the thickness direction of the FG curved panel can be expressed as (Cook et al., 2009):

$$W=\int_v\left[\frac{1}{2}\left\{(u_{,x})^2+(v_{,x})^2+(w_{,x})^2\right\}N_x+\frac{1}{2}\left\{(u_{,y})^2+(v_{,y})^2+(w_{,y})^2\right\}N_y+\left\{u_{,x}\,u_{,y}+v_{,x}\,v_{,y}+w_{,x}\,w_{,y}\right\}N_{xy}\right]\mathrm{d}v \tag{19}$$

where, $\left\{N_x\quad N_y\quad N_{xy}\right\}^T=\left(Q_{11}+Q_{12}\right)\left\{1\quad 1\quad 0\right\}^T\alpha\Delta T$ is the thermal force resultant.

$$W=\frac{1}{2}\iint\left[\left\{\varepsilon_G\right\}^T\left[D_G\right]\left\{\varepsilon_G\right\}\right]\mathrm{d}x\,\mathrm{d}y \tag{20}$$

where, $\{\varepsilon_G\} = \{\varepsilon_{xx} \quad \varepsilon_{yy} \quad \varepsilon_{xy}\}$ is the in-plane strain vector and $[D_G]$ is the material property matrix.

The kinetic energy of the FG shell panel can be expressed as

$$T = \frac{1}{2}\int_V \rho\{\dot{\delta}\}^T\{\dot{\delta}\}\,\mathrm{d}V \tag{21}$$

where, ρ and $\{\dot{\delta}\}$ are the mass density and the global velocity vector.

By substituting the Eq. (2) in the Eq. (21), the kinetic energy of the FG curved panel can be written as

$$T = \frac{1}{2}\int_A \left(\int_{-h/2}^{+h/2} \{\dot{\delta}_0\}^T[f]^T\rho[f]\{\dot{\delta}_0\}\,\mathrm{d}z\right)\mathrm{d}A = \frac{1}{2}\int_A \{\dot{\delta}_0\}^T[m]\{\dot{\delta}_0\}\,\mathrm{d}A \tag{22}$$

where, $[m] = \int_{-h/2}^{+h/2}[f]^T\rho[f]\mathrm{d}z$ is the inertia matrix.

2.6 Finite Element Formulation

The present FG panel model is discretized by using a nine noded isoparametric quadrilateral Lagrangian element. The mid-plane displacement vectors can be expressed in terms of nodal field as

$$\{\delta_0\} = \sum_{i=1}^{9} N_i\{\delta_{0_i}\} \tag{23}$$

where, $\{\delta_{0_i}\} = \left[u_{0_i} \;\; v_{0_i} \;\; w_{0_i} \;\; \theta_{x_i} \;\; \theta_{y_i} \;\; u^*_{0_i} \;\; v^*_{0_i} \;\; \theta^*_{x_i} \;\; \theta^*_{y_i}\right]^T$ is the nodal displacement vector at i^{th} node and N_i is the shape function for the i^{th} node and mentioned in Cook et al. (2009).

Again, the mid-plane strain vector can be written in terms of nodal displacement vector as

$$\{\varepsilon\} = [B]\{\delta_0\} \text{ and } \{\varepsilon_G\} = [B_G]\{\delta_0\} \tag{24}$$

where, B and $[B_G]$ are the product form of differential operator matrix and corresponding shape functions for the mid-plane and in-plane strain terms, respectively.

2.7 Governing equation

The desired free vibration governing equation of the FG curved panel is obtained using Hamilton's principle and expressed as

$$\delta\int_{t_1}^{t_2}\left[T - \left(U + W\right)\right]\mathrm{d}t = 0 \tag{25}$$

The final form of the vibrated FG curved panel under thermal environment can be obtained by substituting Eq. (18-24) in the Eq. (25) and conceded as:

$$\left[M\right]\left\{\ddot{\delta}\right\}+\left(\left[K\right]+\left[K_G\right]\right)\left\{\delta\right\}=0 \tag{26}$$

where,
$\left[M\right]=\left[N\right]^T\left[m\right]\left[N\right]$ is the system mass matrix,
$[K]=[B]^T[D][B]$ is the system stiffness matrix and
$[K_G]=[B_G]^T[D_G][B_G]$ is the geometric stiffness matrix.
Now, Eq. (26) is rearranged to obtain the eigenvalue type equation and presented as

$$\left(\left(\left[K\right]+\left[K_G\right]\right)-\omega^2\left[M\right]\right)\Delta=0 \tag{27}$$

where, ω is the natural frequency and Δ is the corresponding eigenvectors. In the present analysis, the natural frequency is non-dimensionalized using the following formula

$$\bar{\omega}=\omega\left(a^2/h\right)\sqrt{\left(1-v_m^2\right)\rho_m/E_0} \tag{28}$$

where, E_0 denotes the Young's modulus of metal at ambient temperature, i.e., $T=300$ K.

3 NUMERICAL RESULTS AND DISCUSSIONS

In this section, the thermal free vibration behaviour of simply-supported FG curved shell panels are examined under uniform and non-uniform thermal loadings. The FGM constituents are assumed to be temperature dependent as presented in Table 2. The responses are computed through a homemade computer code developed in MATLAB based on the proposed finite element formulation. The convergence behaviour of the numerical model has been checked and the responses are compared with that to the available published results. Finally, some new numerical experiments are examined for different geometrical parameters to show the effectiveness of the present developed model.

3.1 Convergence and comparison study

As a first step, the convergence behaviour of simply-supported FG ($ZrO_2/\ Ti\text{-}6Al\text{-}4V$) flat panel ($a=0.2$ m, $a/h=8$) is computed for different mesh refinement. The non-dimensional fundamental frequency parameter $\left(\bar{\omega}=\omega\left(a^2/h\right)\sqrt{\left(1-v_m^2\right)\rho_m/E_0}\right)$ is computed for different power-law indices ($n=0,\ 0.5,\ 1,\ 2,\ \infty$) and presented in Figure 2. It is observed from the graph that the present model is showing good convergence rate with mesh refinement for all possible cases are investigated and a (6×6) mesh is sufficient to compute the desired frequency responses further.

In order to show the validity of the present developed model, a simply-supported square FG ($ZrO_2/\ Ti\text{-}6Al\text{-}4V$) flat panel is analysed for four different values of the power-law indices ($n=0$, 0.5, 1 and 2) under nonlinear temperature field as shown in Figure 3. The material properties and geometrical parameters are same to be Huang and Shen (2004) as in Table 2. The present results

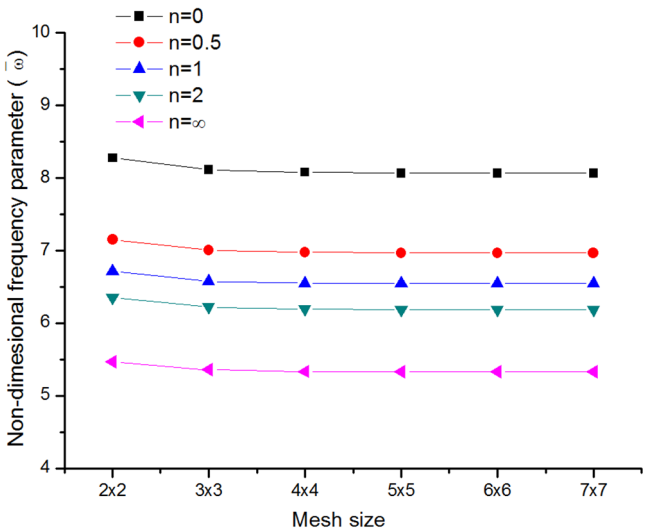

Figure 2: Convergence rate of frequency parameter of a square simply-supported FG flat panel.

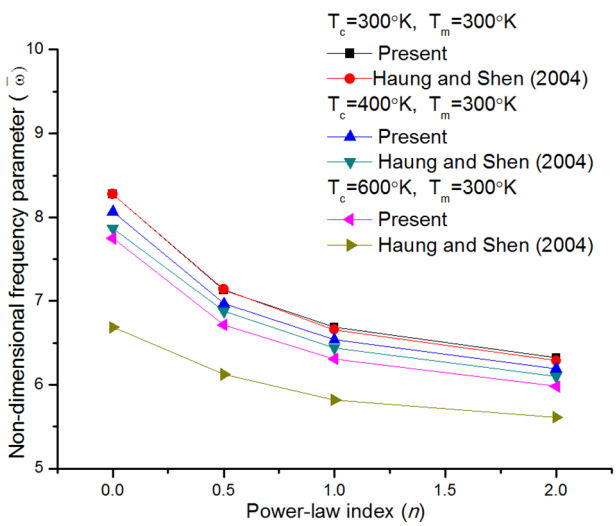

Figure 3: Comparison of frequency parameter of FG flat panel under thermal environment ($a = 0.2$ m, $a/h = 8$).

are showing very good agreement with that to the analytical solutions except $n = 0$ (within 14%) i.e., ceramic rich FG plate, when the structure exposed to the nonlinear temperature distribution ($T_c = 600$ K and $T_m = 300$ K).

Now, another problem has been solved to show the capabilities of the present model to solve curved panel structure. The frequency responses $\left(\bar{\omega} = \omega\left(a^2/h\right)\sqrt{12\left(1-\upsilon_m^2\right)\rho_m/E_m}\right)$ of simply-supported FG spherical/cylindrical shell panels are computed for three curvature ratios ($R/a = 5$, 10 and 50) and three power-law indices ($n = 0$, 0.2 and 10) and shown in Table 3. The top and bottom surfaces of the FG panel are taken as alumina (Al_2O_3) and aluminium (Al), respectively. The material properties are taken same as given in Pradyumna and Bandyopadhyay (2008). The present results are showing good agreement with that of the reference.

Curvature ratio (R/a)		Cylindrical panel			Spherical panel		
	Power-law index (n)	0	0.2	10	0	0.2	10
5	Present	42.658	37.225	19.204	44.405	38.794	19.856
	Pradyumna and Bandyopadhya (2008)	42.254	40.162	19.389	44.007	41.778	20.469
10	Present	42.298	36.906	19.088	42.747	37.302	19.244
	Pradyumna and Bandyopadhya (2008)	41.908	39.847	19.156	42.357	40.260	19.435
50	Present	42.182	36.810	19.061	42.200	36.823	19.063
	Pradyumna and Bandyopadhya (2008)	41.796	39.746	19.081	41.814	39.762	19.092

Table 3: Non-dimensional frequency parameters of simply-supported FG (Al/Al_2O_3) cylindrical/spherical shell panels for different curvature ratios and power-index índices.

3.2 Numerical examples

In this section, some new examples have been solved to demonstrate the influence of different parameters on the frequency responses of FG flat/curved panels under thermal environment. The frequency responses are computed in non-dimensionalized form $\left(\bar{\omega} = \omega\left(a^2/h\right)\sqrt{\left(1-v_m^2\right)\rho_m/E_0}\right)$ throughout the analysis if not stated otherwise. The responses are evaluated for different parameters such as the thickness ratios (a/h), the curvature ratios (R/a), the power-law indices (n) and the aspect ratios (a/b) and three temperature load variation (TD-I, TD-II and TD-III). If not stated otherwise, the results are computed throughout the analysis by setting the geometrical and the material parameters as $R/a = 5$, $a/h = 100$, $n = 2$ and $a/b = 1$. The top and bottom temperatures are taken as $T_c = 300$, 400, 500, 600, 700 K and $T_m = 300$ K, respectively.

3.2.1 Effect of power-law index

It is well known that the FG structure properties greatly depend on the power-law indices, and it also decides the distribution of each constituent across the thickness. Figures 4 and 5 show the frequency responses of the simply-supported square FG flat and curved (spherical, cylindrical, hyperbolic and elliptical) panels for three different power-law indices ($n = 0$, 1, 2) under three thermal environments (TD-I, TD-II and TD-III). It is clear from the figures that, the frequency parameters are decreasing as the power-law indices increase for each shell geometries. It is also interesting to note that the frequency responses are showing descending trend from ceramic rich to metal rich FG structure. It is because the ceramic materials are well known for their high stiffness in comparison to the metal counterpart.

3.2.2 Effect of thickness ratio

The thickness ratio is the essential geometrical parameter for any structural analysis. In this example, the effect of the thickness ratio on the frequency responses are examined. The responses are computed for simply-supported square FG flat/curved panels. Figures 6 and 7 are showing the frequency responses of three different thickness ratios ($a/h = 5$, 20, 100) under three thermal fields as discussed. It is observed that, the frequency parameters are showing increasing type of behaviour as the thickness ratio increase for all the cases irrespective of geometry and temperature field. It is due to the fact that, as the thickness ratio increases the FG panel becomes thin and it has less structural stiffness as compared to thick panels.

3.2.3 Effect of aspect ratio

It is well known that the aspect ratio is one of the major parameters in structural design and it also affect the structural responses considerably. In this example, the effect of the aspect ratio on the frequency responses of FG panel has been analysed for different geometries. Figures 8 and 9 illustrate the variation of frequency responses of the simply-supported FG panels for three different panel configurations, i.e., $a/b = 1.5$, 2 and 2.5. It can be seen clearly that the frequency parameters are increasing as the aspect ratio increases because the panels with large aspect ratios are comparatively stiffer.

3.2.4 Effect of curvature ratio

The curved panel is mainly characterised by the radius of curvature. In order to examine the effect of curvature ratio, the frequency responses of different shell geometries (spherical, cylindrical, hyperbolic and elliptical) are computed for three different values of curvature ratio ($R/a = 10$, 20 and 50) and plotted in Figure 10(a)-(d). The frequency parameters are decreasing as the curvature ratio increases, i.e., in the order of $R/a = 10$, 20 and 50. It is because, as the curvature ratio of any curved panel increases, it approaches to flatness and the flat panels have less membrane energy as compared to the curved one. It is also noted that curvature effect is predominent in case of spherical panel.

3.2.5 Effect of temperature variation

It is well known that the FG structures are more efficient in elevated thermal environment conditions as compared to the laminated structures. In addition, the mechanical properties of FGM constituents, i.e., the metal and the ceramic, are well affected due to the elevated thermal environment. In order to show the effect of temperature on the frequency responses of the FG panel structure, the frequency parameters are computed under three different temperature load (TD-I, TD-II, TD-III) and presented in Figures 4-10. The responses are computed for five different temperatures ($T_c = 300$, 400, 500, 600, 700 K) across the thickness of the FG panel. It is observed from the figures that the frequency parameters are decreasing with the temperature increment, i.e., the FG structures become flexible at higher temperatures. It is also interesting to note that the frequency parameters are increasing in ascending order from TD-I, TD-II and TD-III, respectively.

3.2.6 Effect of shell geometry

The man made shells are classified based on their curvature rather than the load bearing capacity. Here, the frequency responses of different shell geometries (flat, spherical, cylindrical, hyperbolic and elliptical panels) are investigated under three different thermal environment and presented in Figures 4-10. It is clear from the Figures 4-7 that, the frequency responses are increasing progressively following the order of flat, cylindrical, elliptical, hyperbolic and spherical shell panel. The trends are deviating in Figures 8-10, where the elliptical panels are showing higher frequencies in comparison to the hyperbolic panel. The results also indicate that the curved panels are stiffer in comparison to that of the flat panel.

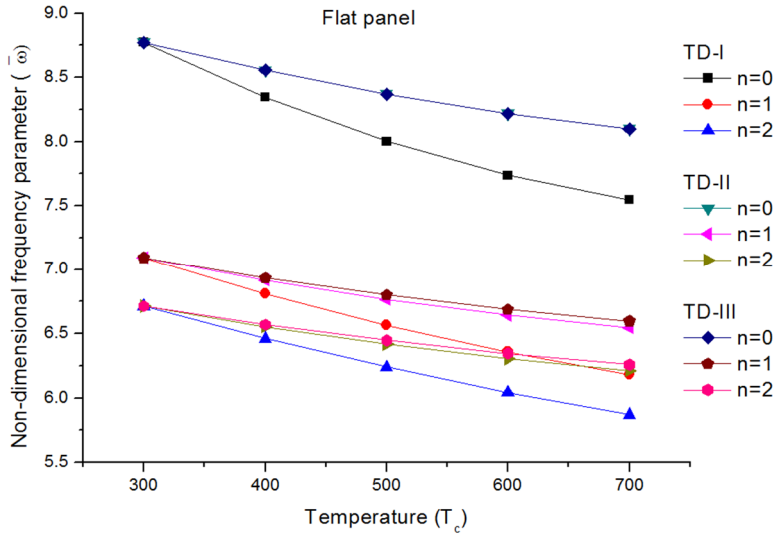

Figure 4: Effect of power-law index on the frequency parameters of FG flat panel under various temperature fields.

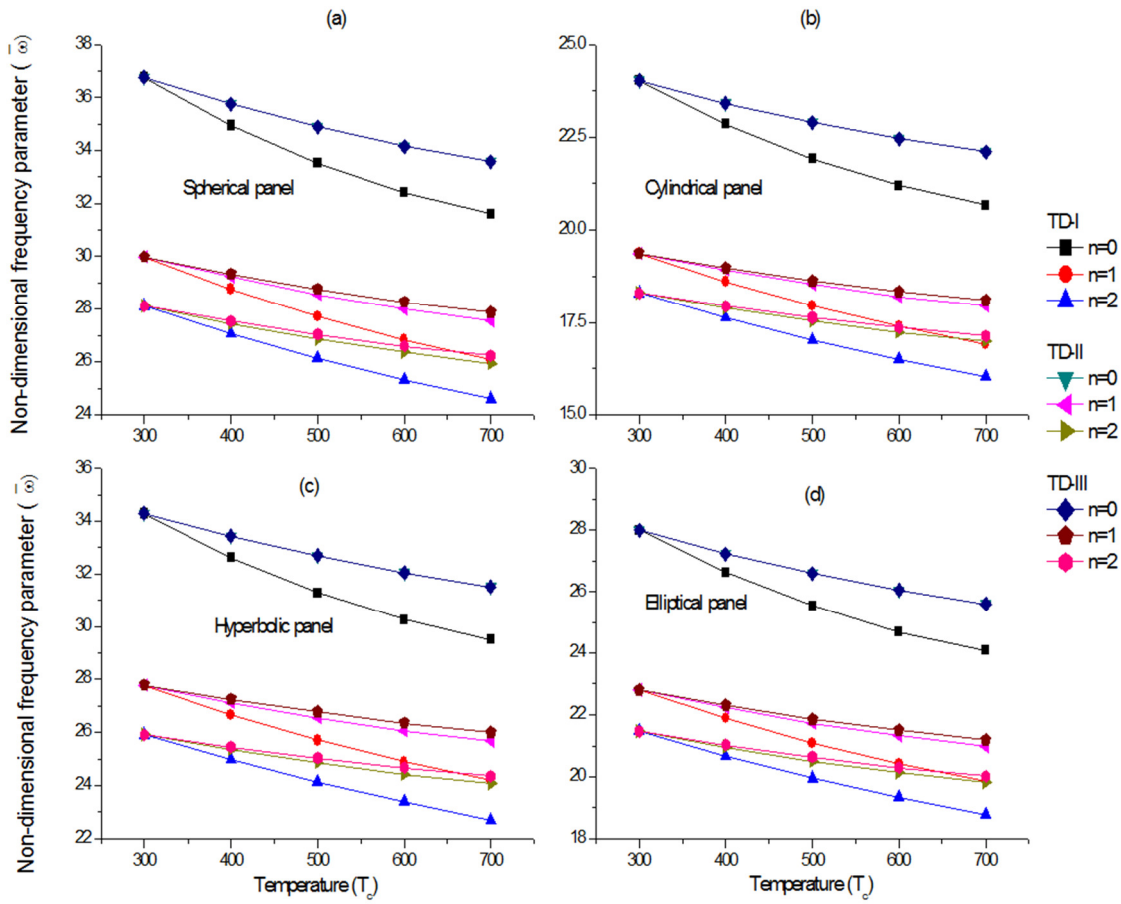

Figure 5(a)-(d): Effect of power-law index on the frequency parameters of FG panels under various temperature fields.

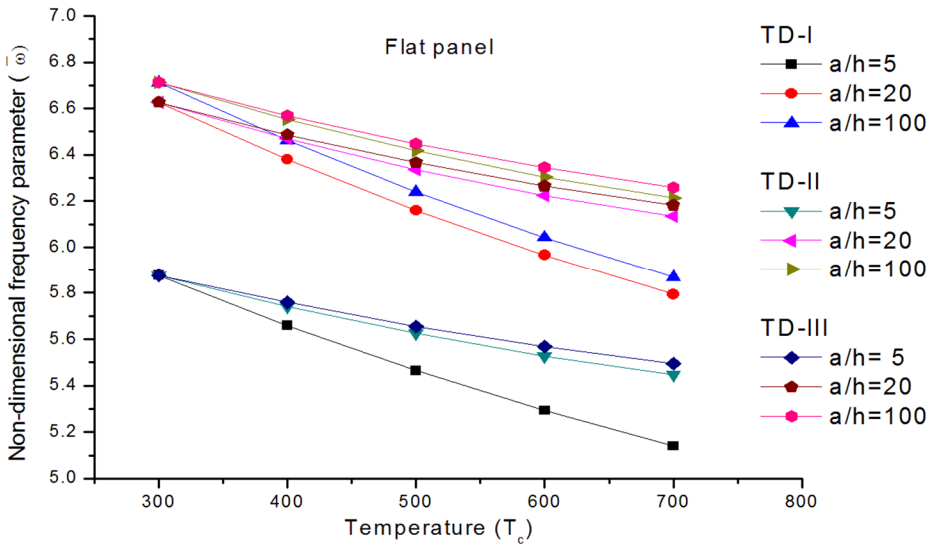

Figure 6: Effect of thickness ratio on the frequency parameters of FG flat panel under various temperature fields.

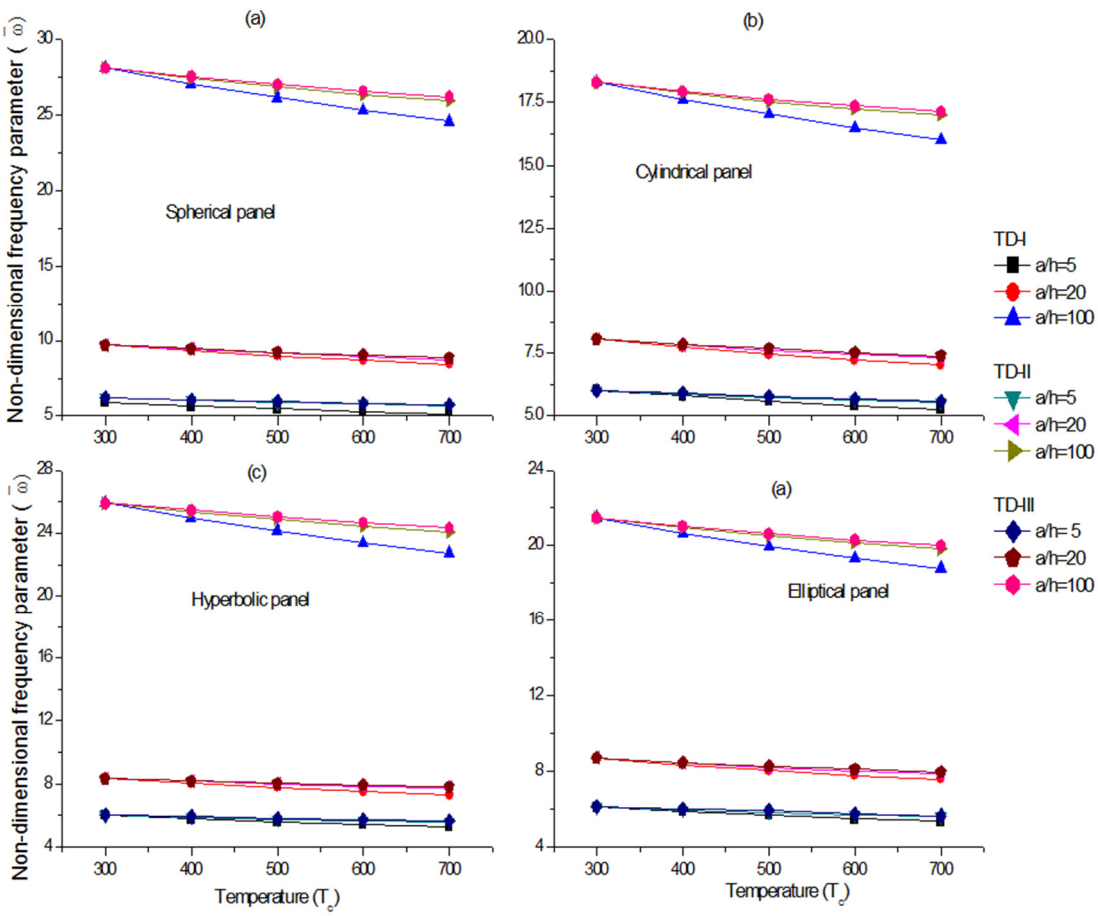

Figure 7(a)-(d): Effect of thickness ratio on the frequency parameters of FG panel under various temperature fields.

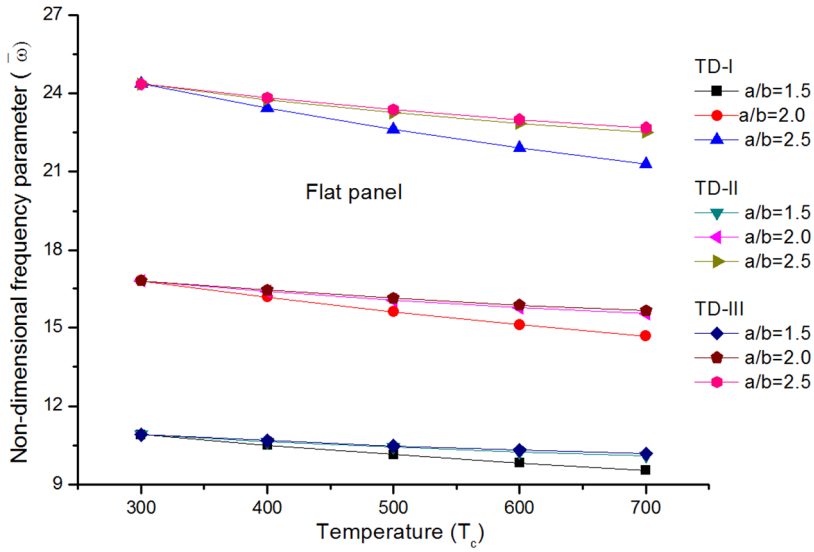

Figure 8: Effect of aspect ratio on the frequency parameters of FG flat panel under various temperature fields

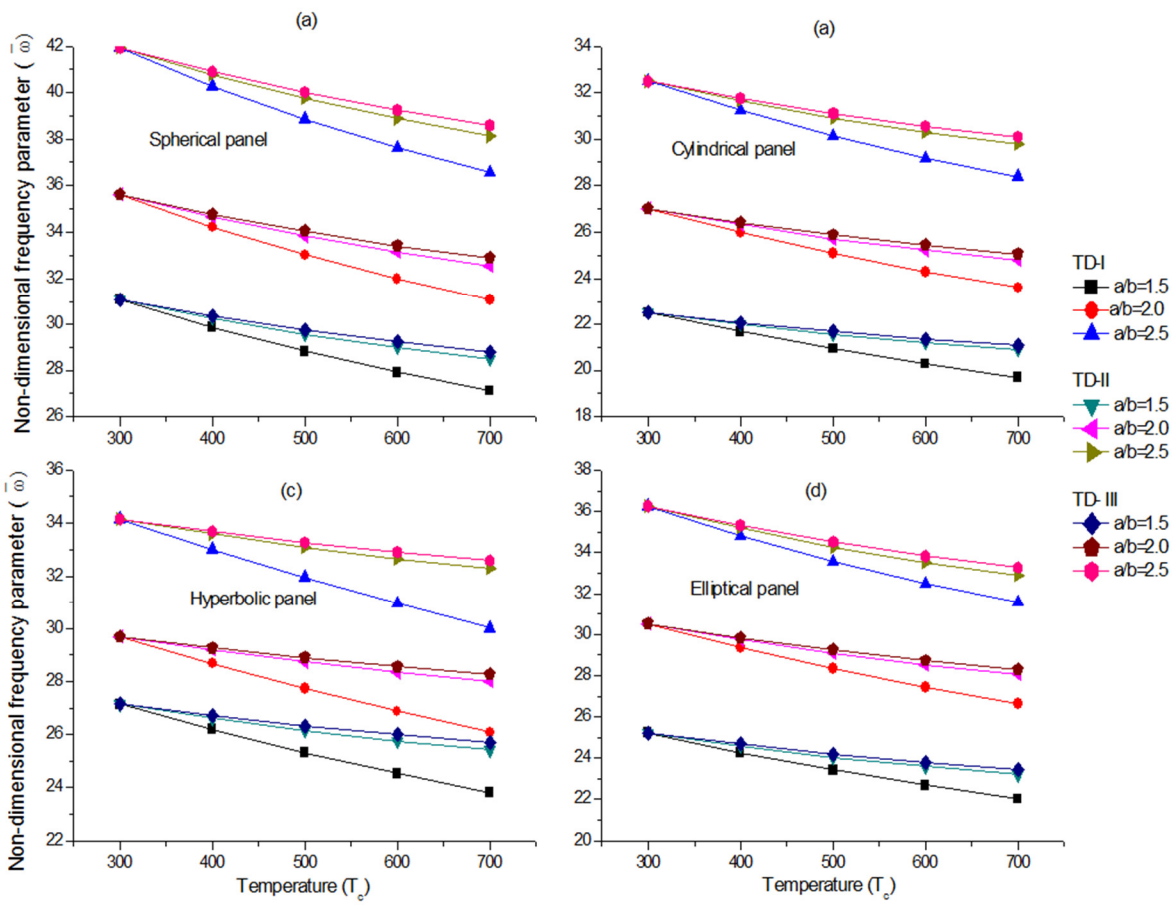

Figure 9(a)-(d): Effect of aspect ratio on the frequency parameters of FG panels under various temperature fields.

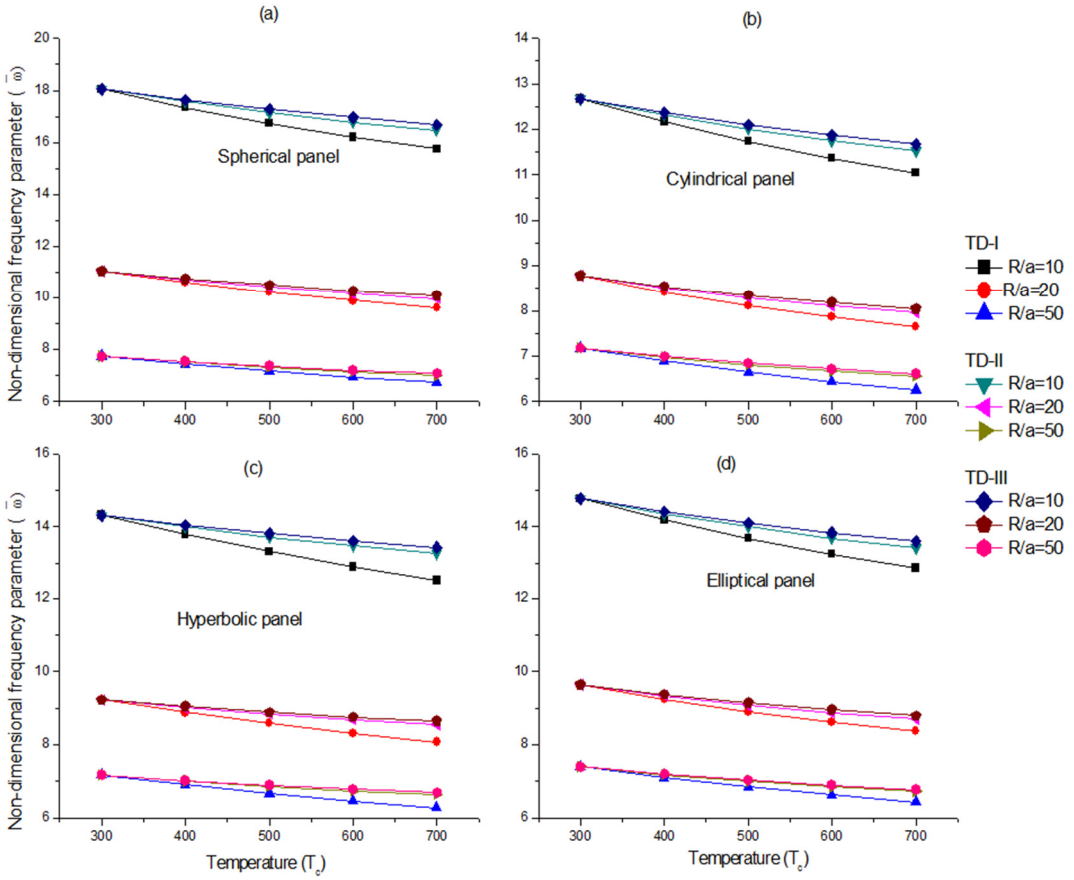

Figure 10(a)-(d): Effect of curvature ratio on the frequency parameters of FG panels under various temperature fields

4 CONCLUSIONS

The free vibration responses of simply-supported FG flat/curved shell panels are examined under elevated thermal environments. The responses are computed numerically using a generalised mathematical model developed in the framework of the HSDT mid-plane kinematics in conjunction with finite element method under three different temperature loading conditions (uniform, linear and nonlinear). In order to achieve the real life situation, the FGM properties are assumed to be temperature dependent and the effective material properties are computed using Voigt's micromechanical model via power-law distribution of the volume fractions. The desired governing equation of vibrated FG panel structure is obtained using Hamilton's principle. The convergence behaviour of the present numerical model has been computed to show the stability of the numerical results and validated by comparing with the previously published literature. Effects of different geometrical and material parameters on the frequency responses of single/doubly curved and flat panels under uniform, linear and nonlinear thermal fields are examined and discussed in details. The following conclusions are made on the present parametric study on the FG flat/curved shell panels:

- It is observed that, the frequency responses are increasing as the thickness ratio and the aspect ratio increases irrespective of the FG shell panel geometries.

- The frequency responses are decreasing as the power-law indices and the curvature ratios increases.
- The frequency parameter are decreasing with the increase of temperature load for each shell geometries.
- It is also noticed that, the frequency parameters are higher for all the FG shell geometries under nonlinear temperature load distribution in comparison to the uniform and the linear temperature.
- The frequency parameters are maximum and minimum for the spherical and the flat panels, respectively.

References

Alijani, F., Amabili, M., Karagiozis, K., Bakhtiari-Nejad, F., (2011a). Nonlinear vibrations of functionally graded doublcurved shallow shells. Journal of Sound and Vibration 330: 1432–1454.

Alijani, F., Amabili, M., Karagiozis, K., Bakhtiari-Nejad, F., (2011b). Thermal effects on nonlinear vibrations of functionally graded doubly curved. Composite Structures 93: 2541–2553.

Asemi, K., Salami, S.J., Salehi, M., Sadighi, M., (2014). Dynamic and static analysis of FGM skew plates with 3D elasticity based graded finite element modeling. Latin American Journal of Solids and Structures 11: 504–533.

Baferani, A.H., Saidi, A.R., Jomehzadeh, E., (2012). Exact analytical solution for free vibration of functionally graded thin annular sector plates resting on elastic foundation. Journal of Vibration and Control 18(2): 246–267.

Bich, D.H., Duc, N.D., Quan, T.Q., (2014). Nonlinear vibration of imperfect eccentrically stiffened functionally graded double curved shallow shells resting on elastic foundation using the first order shear deformation theory. International Journal of Mechanical Sciences 80: 16–28.

Cook, R.D., Malkus, D.S., Plesha, M.E., Witt, R.J., (2009). Concepts and applications of finite element analysis. John Wiley & Sons, Singapore.

Gibson, L.J., Ashby, M.F., Karam, G.N., Wegst, U., Shercliff, H.R., (1995). Mechanical properties of natural materials. II. Microstructures for mechanical efficiency. Proceedings of the Royal Society A 450: 141-162.

Haddadpour, H., Mahmoudkhani, S., Navazi, H.M., (2007). Free vibration analysis of functionally graded cylindrical shells including thermal effects. Thin-Walled Structures 45: 591–599.

Hosseini-Hashemi, Sh., Taher, H.R.D., Akhavan, H., Omidi, M., (2010). Free vibration of functionally graded rectangular plates using first-order shear deformation plate theory. Applied Mathematical Modelling 34: 1276–1291.

Huang, X.L., Shen, H.S., (2004). Nonlinear vibration and dynamic response of functionally graded plates in thermal environments. International Journal of Solids and Structures 41: 2403–2427.

Javaheri, R., Eslami, M.R., (2002). Thermal buckling of functionally graded plates. AIAA Journal 40: 162–169.

Kar, V.R., Panda, S.K., (2015). Large deformation bending analysis of functionally graded spherical shell using FEM. Structural Engineering and Mechanics 53(4): 661-679.

Koizumi, M., (1993). The concept of FGM, Ceramic Transactions. Functionally Gradient Materials 34: 3–10.

Miyamoto, Y., Kaysser, W.A., Rabin, B.H., Kawasaki, A., Ford, R.G., (1999). Functionally Graded Materials: Design. Processing and Applications. Kluwer Academic, Boston.

Pandya, B.N., Kant, T., (1988). Finite element analysis of laminated composite plates using a higher-order displacement model. Composites Science and Technology 32: 137-155.

Patel, B.P., Gupta, S.S., Loknath, M.S., Kadu, C.P., (2005). Free vibration analysis of functionally graded elliptical cylindrical shells using higher-order theory. Composite Structures 69: 259–270.

Pradyumna, S., Bandyopadhyay, J.N., (2008). Free vibration analysis of functionally graded curved panels using a higher-order finite element formulation. Journal of Sound and Vibration 318: 176–192.

Pradyumna, S., Bandyopadhyay, J.N., (2010). Free vibration and buckling of functionally graded shell panels in thermal environments. International Journal of Structural Stability and Dynamics 10(5): 1031-1053.

Pradyumna, S., Nanda, N., (2013). Geometrically nonlinear transient response of functionally graded shell panels with initial geometric imperfection. Mechanics of Advanced Materials and Structures 20: 217–226.

Pradyumna, S., Nanda, N., Bandyopadhyay, J.N., (2010). Geometrically nonlinear transient analysis of functionally graded shell panels using a higher-order finite element formulation. Journal of Mechanical Engineering Research 2: 39–51.

Rahimia, G.H., Ansari, R., Hemmatnezhada, M., (2011). Vibration of functionally graded cylindrical shells with ring support. Scientia Iranica 18(6): 1313–1320.

Reddy, J.N., Chin, C.D., (1998). Thermomechanical analysis of functionally graded cylinders and plates. Journal of Thermal Stresses 21: 593–626.

Santos, H., Soares, C.M.M., Soares, C.A.M., Reddy, J.N., (2009). A semi-analytical finite element model for the analysis of cylindrical shells made of functionally graded materials. Composite Structures 91: 427–432.

Shen, H.S., (2009). Functionally graded material: Nonlinear analysis of plates & shells. CRC press, Boca Raton.

Shen, H.S., Wang, H., (2014). Nonlinear vibration of shear deformable FGM cylindrical panels resting on elastic foundations in thermal environments. Composites: Part B 60: 167–177.

Sundararajan, N., Prakash, T., Ganapathi, M., (2005). Nonlinear free flexural vibrations of functionally graded rectangular and skew plates under thermal environments. Finite Elements in Analysis and Design 42: 152–168.

Taj, G., Chakrabarti, A., (2013). Dynamic response of functionally graded skew shell panel. Latin American Journal of Solids and Structures 10: 1243–1266.

Talha, M., Singh, B.N., (2011). Large amplitude free flexural vibration analysis of shear deformable FGM plates using nonlinear finite element method. Finite Elements in Analysis and Design 47: 394–401.

Uymaz, B., Aydogdu, M., (2007). Three-dimensional vibration analysis of functionally graded plates under various boundary conditions. Journal of Reinforced Plastics and Composites 26(18): 1847–1863.

Yang, J., Shen, H.S., (2003). Free vibration and parametric resonance of shear deformable functionally graded cylindrical panels. Journal of Sound and Vibration 261: 871–893.

Zhu, P., Zhang, L.W., Liew, K.M., (2014). Geometrically nonlinear thermomechanical analysis of moderately thick functionally graded plates using a local Petrov–Galerkin approach with moving Kriging interpolation. Composite Structures 107: 298–314.